Elucidation of the mechanism of miR-122-5p in mediating FOXO3 injury and apoptosis of mouse cochlear hair cells induced by hydrogen peroxide

JIAJUN CHEN, JIXIN QIN and JIN LIU

Department of Otorhinolaryngology Head and Neck Surgery, Affiliated Hospital of Youjiang Medical College for Nationalities, Baise, Guangxi 533000, P.R. China

Received May 20, 2021; Accepted March 15, 2022

DOI: 10.3892/etm.2022.11362

Abstract. Unveiling the mechanism of miR-122-5p in the mediation of forkhead box O3 (FOXO3) in regards to cochlear hair cell damage provides an effective solution for the treatment of ear hearing disorders. An oxidative stress model using a mouse cochlear hair cell line (HEI-OC1) was established via hydrogen peroxide (H_2O_2). Then HEI-OC1 cells were transfected with miR-122-5p mimic, miR-122-5p inhibitor, and lentiviral vector FOXO3-WT/MUT. Cell viability and apoptosis rate were determined by MTT assay and flow cytometry. Reactive oxygen species (ROS) were observed by confocal laser scanning microscopy. Bcl-2, Bax, capase-3 and c-caspase-9 levels were quantified by western blot analysis and quantitative reverse transcription polymerase chain reaction (RT-qPCR). Enzyme-linked immunosorbent assay (ELISA) was used to detect superoxide dismutase (SOD) and malondialdehyde (MDA) levels, and flow cytometry was performed to measure the mitochondrial membrane potential levels. In the HEI-OC1 oxidative stress model after transfection, the miR-122-5p level was decreased, whereas the FOXO3 level was increased, Moreover, the increased FOXO3 level diminished the cell viability, but promoted cell apoptosis. Apart from this, the Bcl-2 level was downregulated, while levels of Bax, c-caspase-3, c-caspase-9, ROS and MDA were upregulated. Meanwhile, the mitochondrial membrane potential level was also elevated. Overexpression of miR-122-5p was able to partially offset the effects of FOXO3 in the H_2O_2-treated HEI-OC1 cells. Collectively, miR-122-5p restrained the decrease in HEI-OC1 cell viability and apoptosis induced by treatment with H_2O_2.

Correspondence to: Dr Jiajun Chen, Department of Otorhinolaryngology Head and Neck Surgery, Affiliated Hospital of Youjiang Medical College for Nationalities, 18 Zhongshan 2 Road, Baise, Guangxi 533000, P.R. China
E-mail: chenjiajun_cjj1@163.com

Key words: miR-122-5p, FOXO3, H_2O_2, HEI-OC1, oxidative stress

Introduction

Cochlear hair cells, as the mechanoreceptors of the inner ear, are essential to auditory and vestibular function, the loss of which ultimately leads to permanent sensory deficits in mammals (1). Hearing loss, a very frequent sensory disorder in humans, is mainly attributable to cochlear hair cell damage caused by hazardous factors containing ototoxic pharmaceutical agents, excessive noise, aging and genetic disorders. Oxidative stress and high levels of reactive oxygen species (ROS) have an involvement with drug- and noise-induced, and age-related hearing injury, while cisplatin, aminoglycosides and continuous noise can result in high level of ROS production in cochlear hair cells, thereby inducing cell apoptosis (2). Cochlear hair cells do not spontaneously regenerate following loss or damage, due to the limitation of regenerative capacity of vestibular organs (3). Therefore, it will be of great significance to fathom out the pathways and molecular regulators involved in the pathogenesis of ROS-related hair cell cytotoxicity for the advancement of therapies toward functional restoration.

MicroRNAs (miRNAs/miRs), an important class of small non-coding RNAs, bind to target mRNAs and subsequently inhibit protein expression through mRNA degradation or translational inhibition (4). miRNAs play pivotal roles in various important biological processes as well as in the development and progression of various human diseases, where one miRNA can exert impacts on multiple target genes, and multiple miRNAs in turn can also synergistically act on one target gene (5,6). Several research studies have manifested that miR-122-5p is associated with many diseases, especially tumors or cancers, including colorectal cancer, melanoma, gastric cancer, lung cancer and cervical cancer (7-12). In addition, plasma miRNA-122-5p has been identified as a potential biomarker for liver injury among chronic hepatitis B (CHB) patients with persistently normal alanine aminotransferase (PNALT) levels (13), and transient ischemic attack in rats (14). Zhou *et al* (15) demonstrated that miRNA-122-5p promotes the proliferation and DNA synthesis and represses the early apoptosis of human spermatogonial stem cells via targeting CBL and competing with lncRNA CASC7. Peng *et al* (16) reported that lncRNA XIST relieves hypoxia-induced injury in H9c2 cardiomyocytes via targeting the miR-122-5p/FOXP2

axis. Furthermore, many miRNAs also play vital roles in the development of cochlea inner ear hair cells and may be pivotal regulators in the process of hearing loss (17-21). Wang *et al* (2) demonstrated that tert-butyl hydroperoxide (t-BHP) promotes the production of ROS, and miR-122-5p expression was significantly downregulated in House Ear Institute-Organ of Corti 1 (HEI-OC1) cells. miR-122-5p was found to inhibit cell apoptosis and facilitate tumor progression by directly targeting forkhead box O3 (FOXO3) in α-fetoprotein (AFP)-producing gastric cancer (AFPGC) (7). Moreover, FOXO3 expression was found to be increased in the inner ear hair cells during cisplatin treatment *in vitro* (22).

Therefore, we hypothesized that miR-122-5p can directly target FOXO3 to regulate the viability and apoptosis of cochlear hair cells under oxidative stress condition. The oxidative damage model was established in HEI-OC1 cells to elucidate the role and mechanism of miR-122-5p, hoping to provide more treatment options for hearing disorders. Our present study demonstrated that miR-122-5p overexpression attenuated the H_2O_2-induced damage in mouse cochlear hair cells by directly regulating FOXO3.

Materials and methods

Cell culture. The House Ear Institute-Organ of Corti 1 (HEI-OC1) cell line was obtained from the Medical Experimental Center of Guangzhou Red Cross Hospital (China). High-glucose Dulbecco's modified Eagle's medium (DMEM) (30-2002, American Type Culture Collection, Beijing, China) supplemented with 10% fetal bovine serum (FBS; C0257, Beyotime Institute of Biotechnology) was used to culture the HEI-OC1 cells at 33˚C in a humidified incubator with 5% CO_2.

Cell transfection. The miR-122-5p mimic (M; 5'-UGGAGU GACAAUGGUGUUUG-3'), mimic control (MC; 5'-UUC UCCGAACGUGUCACGUTT-3') and FOXO3 lentivirus were obtained by transfection of 293T cells (ab266546, Abcam) with pPACKH1 Lentivector Packaging Kit (US SBI Co.). The FOXO3 overexpression vector was constructed by cloning the cDNA of mouse FOXO3 into the pPACKH1 lentivector. The HEI-OC1 cells were placed into a 24-well plate at the density of $1x10^5$ cells/well. The density of the cells during lentiviral transfection was ~$2x10^5$ cells/well. The next day, the original medium was replaced by 2 ml of fresh medium containing 6 μg/ml polybrene, followed by the addition of an appropriate amount of the viral suspension. Subsequently, the membrane was incubated at 37˚C. After 4 h, another 2 ml of fresh medium was supplemented to dilute the polybrene. Following continuous culture for 24 h, the virus-containing medium was substituted with fresh medium, which was then used to continuously culture the cells. Four days later, the infected cells were collected by trypsinization and replated on a new 100-mm dish. While cell confluence reached about 30%, the culture medium was replaced by fresh medium containing 1 μg/μl puromycin for colony selection of stable transfected cells. The medium was changed every 3 day, and colonies were chosen and expanded for subsequent experiments after section. A blank vector lentivirus was used as a negative control (NC).

Oxidative stress exposure and grouping. HEI-OC1 cells were exposed to 50 μM hydrogen peroxide (H_2O_2) for 1 h post transfection to mimic oxidative stress condition, as previously reported (10). To unveil the effect of miR-122-5p in HEI-OC1 cells under oxidative stress, HEI-OC1 cells were assigned into four groups: Blank, Model, Model+MC and Model+M groups. Similarly, in order to explore the roles of miR-122-5p and FOXO3 in HEI-OC1 cells under oxidative stress, HEI-OC1 cells were divided into seven groups: Blank, Model, Model+MC, Model+M, Model+NC, Model+FOXO3 and Model+M+FOXO3 groups. The specific treatment of cells in the various groups was shown as follows. In the Blank group, HEI-OC1 cells were only incubated with medium; in the Model group, HEI-OC1 cells were exposed to 50 μM H_2O_2 for 1 h; in the Model+MC group, HEI-OC1 cells were exposed to 50 μM H_2O_2 for 1 h and then transfected with the mimic control; in the Model+M group, HEI-OC1 cells were exposed to 50 μM H_2O_2 for 1 h and then transfected with miR-122-5p mimic; in the Model+NC group, HEI-OC1 cells were exposed to 50 μM H_2O_2 for 1 h and then transfected with the blank vector lentivirus; in the Model+FOXO3 group: HEI-OC1 cells were exposed to 50 μM H_2O_2 for 1 h and then transfected with the FOXO3 lentivirus; in the Model+M+FOXO3 group: HEI-OC1 cells were exposed to 50 μM H_2O_2 for 1 h and then co-transfected with the miR-122-5p mimic and FOXO3 lentivirus.

Dual luciferase reporter assays. TargetScan V7.2 (www.targetscan.org/vert_72/) was used to explore the targets of miR-122-5p. HEI-OC1 cells ($1x10^5$) were seeded to a 24-well plate and then incubated overnight. Next, pcDNA3.1 FOXO3-wild-type (WT; 5'-TGAAGGCCTCGGTCACAC TCCA-3') or pcDNA3.1 FOXO3-mutant (MUT; 5'-TGC AAGGCCTCGGTCGACAAGTTG-3') and miR-122-5p M (5'-TGGAGTGTGACAATGGTGTTTG-3'; HMI1002, MilliporeSigma, USA) were co-transfected into 293T cells (12022001, MilliporeSigma, USA) with Lipofectamine 2000 (11668019, Thermo Fisher Scientific, Inc.).

Subsequently, 100 μl transfected cells were placed in a 96-well plate and then added together with 100 μl Dual-Lumi™ firefly luciferase assay reagent or 100 μl Dual-Lumi™ *Renilla* luciferase assay working solution that was derived from the dual luciferase reporter gene assay kit (RG088M, Beyotime Institute of Biotechnology). After being mixed well, the cells were incubated at room temperature (~25˚C) for 10 min. Finally, cell luciferase was determined with the dual luciferase reporter assay system (Promega Corp.). In this research, dual luciferase reporter assays were performed three times.

Reverse transcription quantitative polymerase chain reaction (RT-qPCR). After being exposed to 50 μM H_2O_2 for 1 h post transfection, HEI-OC1 cells were collected for RNA extraction using the RNAeasy kit (R0027; Beyotime Institute of Biotechnology) and the miRNA was extracted by the RNAeasy kit (R0028; Beyotime Institute of Biotechnology). RNA was detected using a UV spectrophotometer (DR6000; Hash) and then reversed by the reverse transcription kit (D7168L; Beyotime Institute of Biotechnology) for cDNA synthesis. Finally, cDNA, as a template, was amplified using a real-time fluorescence quantitative PCR instrument (ABI 7500; Thermo

Fisher Scientific, Inc.). The conditions of amplification are listed as follows: pre-denaturation at 95˚C for 10 sec, followed by 30 cycles of denaturation at 95˚C for 5 sec and 60˚C for 25 sec, and an elongation at 70˚C for 30 min. The forward and reverse primers for the miR-122-5p sequence, according to Primer3Plus (http://www.primer3plus.com/cgi-bin/dev/primer3plus.cgi), were 5'-TGTGACAATGGTGTTTGGTCG-3' and 5'-TGTCGTGGAGTCGGCAATTG-3'; FOXO3 forward primer was 5'-TCACGCACCAATTCTAACGC-3', and the universal primer was 5'-CACGGCTTGCTTACTGAAGG-3'. U6 (forward primer 5'-CTCGCTTCGGCAGCACA-3' and reverse primer 5'-AACGCTTCACGAATTTGCGT-3') was used as the reference gene, and the $2^{-\Delta\Delta Cq}$ method was utilized to calculate the expression level (23).

Western blot (WB) analysis. Cells ($1x10^6$-$1x10^7$) were taken from each group as samples, and then washed with phosphate-buffered saline (PBS; C0221A; Beyotime Institute of Biotechnology). Next, the cell samples were added with 0.5 ml total protein extraction reagent to extract the total protein. Based on the instructions of the total protein extraction kit (W034-1-1; Nanjing Jiancheng Bioengineering Institute, http://www.njjcbio.com), the protein concentrations were determined. Subsequently, the proteins (20 μg) were loaded and separated by 10% sodium dodecyl sulfate-polyacrylamide gel electrophoresis (SDS-PAGE). After the proteins were transferred to the nitrocellulose membrane and polyvinylidene fluoride (PVDF) membrane, the membranes were cultured in blocking solution (P0023B, 100 ml; Beyotime Institute of Biotechnology) at room temperature for 1 h. After that, anti-Bax (SAB3500343, 23 kDa, 1:1,000; Sigma-Adrich; Merck KGaA), anti-caspase 3 (ab49822, 17 kDa, 1:1,000, Abcam), Bcl-2 (ab182858, 26 kDa, 1:800, Abcam), anti-caspase-9 (SAB4503334, 46 kDa, 1:1,000, Sigma-Adrich; Merck KGaA) and anti-FOXO3 (ab23683, 90 kDa, 1:500, Abcam) antibodies were added to the membranes followed by incubation for 1 h. Later, the membranes were removed and washed three times with Tris-buffered saline Tween (TBST; P0231; Beyotime Institute of Biotechnology) at room temperature. To bind the primary antibody, the membranes were supplemented with horseradish peroxidase (HRP)-labeled secondary antibody (A0201, Beyotime Institute of Biotechnology) and then incubated at room temperature for 1 h. Finally, the membranes were rinsed with TBST (P0231; Beyotime Institute of Biotechnology) again. Finally, bands were visualized using enhanced chemiluminescence (ECL), and then quantified with Image Lab 4.1 software (Bio-Rad Laboratories, Inc.). During this process, glyceraldehyde-3-phosphate dehydrogenase (GAPDH) was utilized as an internal reference. The raw data of all western blot analyses have been provided in the supplementary materials.

Cell viability assay. After being transfected, cells ($2x10^3$ cells/well) were seeded into a 96-well plate and maintained at 37˚C in 100 μl of culture medium. After transfection for 24, 48, 72 and 96 h, the cells in each well were supplemented with 3-(4,5)-dimethylthiahiazo(-z-yl)-3,5-di-phenytetrazoliumromide (MTT, 5 mg/ml, 30 μl; M2128; Sigma-Adrich; Merck KGaA). Then, after removing the medium, 100 μl of dimethyl sulfoxide (DMSO; D2650; Sigma-Adrich; Merck KGaA) was added to solubilize the crystals, and the absorbance was measured at 450 nm. The cell viability assay was independently performed at least three times.

Flow cytometry. Firstly, the cells were resuspended in 400 μl of binding buffer (1X) at a concentration of $1x10^6$ cells/ml. After the addition of 5 μl Annexin V-FITC (APOAF-20TST; Sigma-Adrich; Merck KGaA), the cells were cultivated at room temperature for 15 min in the dark, followed by continuous incubation with 10 μl of propidium iodide (PI; P4170; Sigma-Adrich; Merck KGaA) for 5 min. Finally, the fluorescence intensity of cells in each group was measured by flow cytometry (Fortessa X-20; Bio-Rad Laboratories, Inc. USA).

Enzyme-linked immunosorbent assay (ELISA). Diluted cell samples (100 μl) were transferred to a 96-well plate and incubated at room temperature for 2.5 h. After being rinsed 4 times with 1X washing buffer, each well of the plate was added together with 100 μl of prepared biotin conjugate, followed by 1 h of incubation at room temperature with gentle shaking. After rinsing 4 times with 1X washing buffer, the plate was supplemented with 100 μl of the prepared streptavidin-HRP solution, and incubated at room temperature for 45 min with gentle shaking. Following that, the solution was discarded, the plate was rinsed with 1X washing buffer for another 4 times, and each well was added with 100 μl of TMB substrate. Subsequently, the plate was incubated at room temperature for 30 min in the dark with gentle shaking. Afterwards, 50 μl of stop solution was placed into each well, and the side of the plate was tapped to mix the solution well. Finally, 200 μl of supernatant was collected and then added to the 96-well plate, subsequent to which the absorbance was measured at 532 nm using a microplate reader (Z742711-1EA; Sigma-Adrich; Merck KGaA). Lipid peroxidation assay kit (MDA; A0031-2) and superoxide dismutase assay kit (SOD; A001-3-2) applied in the whole processes were purchased from Nanjing Jiancheng Bioengineering Institute.

Confocal laser scanning microscopy analysis. After exposure to 50 μM H_2O_2 for 1 h, the HEI-OC1 cells were cultured using the ROS Assay Kit (S0033S; Beyotime Institute of Biotechnology), added together with an appropriate volume of diluted 2',7'-dichlorodihydrofluorescein diacetate (DCFH-DA; 1:1,000), and then inoculated to a 6-well plate. Then cells were separately dyed by Mito-SOX Red (C1049-50 μg; Beyotime Institute of Biotechnology) staining with a final concentration of 4 μmol/l at 37˚C for 10 min in the dark or CM-H_2DCFDA (S0033S; Beyotime Institute of Biotechnology) staining at a final concentration of 5 μmol/l at 37˚C for 30 min in the dark. After washing three times with PBS (C0221A; Beyotime Institute of Biotechnology), the cells were captured by laser confocal microscope (LSM800; Zeiss) at different excitation wavelengths (510 nm/488 nm) and different emission wavelengths (580/515 nm), and fluorescence images were captured.

Flow cytometry to detect the mitochondrial membrane potential level. The mitochondrial membrane potential level was measured with the mitochondrial membrane potential

assay kit (JC-1; C2006; Beyotime Institute of Biotechnology). Concretely, the cells were collected and then seeded to each cell of a 6-well plate, with the culture medium aspirated. Following being washed once with PBS (C0221A; Beyotime Institute of Biotechnology), the cells were added together with 1 ml of fresh cell culture medium which contained serum and phenol red. Subsequently, 1 ml JC-1 staining working solution was added and mixed well to cultivate the cells in an incubator at 37˚C for 20 min. During the incubation period, an appropriate amount of JC-1 staining buffer (1X) was prepared according to the ratio of 4 ml distilled water per 1 ml JC-1 staining buffer (5X), and placed in an ice bath. After incubation at 37˚C, the supernatant was aspirated and the cells were washed twice with JC-1 staining buffer (1X). Finally, the cells were supplemented with 2 ml of cell culture medium containing serum and phenol red and observed using a flow cytometer (Fortessa X-20; Bio-Rad Laboratories, Inc.).

Statistical analyses. SPSS version 17.0 (SPSS Inc.) was adopted to analyze the statistical data from this research, and these data are represented as the mean ± standard deviation (SD). The Student's t-test or one way analysis of variance (one-way ANOVA) with post hoc Tukey test was utilized to gauge the results for two or multiple groups. P<0.05 was considered as indicative of a statistically significant difference.

Results

miR-122-5p promotes the viability but inhibits the apoptosis of H_2O_2-induced HEI-OC1 cells. HEI-OC1 cells were exposed to 50 μM H_2O_2 for 1 h (Model group), and subsequently, the expression level of miR-122-5p was observed to be significantly decreased relative to that of the Blank group (Fig. 1A, P<0.001). As shown in Fig. 1B, miR-122-5p mimic (M) transfection significantly increased the level of miR-122-5p in the HEI-OC1 cells (P<0.001). Compared with that of the Blank group, the cell viability of the Model group showed a significant decrease at 24, 48 and 72 h (Fig. 1C, P<0.05). In comparison with that of the Model+mimic control (MC) group, the cell viability of the Model+M group was significantly elevated at 24, 48 and 72 h (Fig. 1C, P<0.05). Additionally, the Model group exhibited a significant increase in the apoptosis rate as compared with Blank group, while the Model+M group had a significantly lower apoptosis rate than the Model+MC group (Fig. 1D, P<0.001). These findings indicated that oxidative stress reduced the cell viability but promoted cell apoptosis. Moreover, high expression of miR-122-5p reversed the effects of the oxidative stress on the viability and apoptosis of the HEI-OC1 cells.

High expression of miR-122-5p partially offsets the effect of H_2O_2 on the expression levels of apoptosis-related proteins in HEI-OC1 cells. The results revealed that compared with the Blank group, the protein expression levels of Bax, cleaved (C)-caspase-3, and C-caspase-9 in the Model group were significantly upregulated (Fig. 2A, C-E, P<0.01) as well as the RNA level of Bax (Fig. 2G, P<0.01), while that of Bcl-2 was downregulated at both the protein (Fig. 2A and B, P<0.001) and RNA level (Fig. 2F, P<0.001). Compared with the Model+MC group, the expression levels of Bax, C-caspase-3, and C-caspase-9 were significantly downregulated (Fig. 2A, C-E and G, P<0.05), while the Bcl-2 level was significantly upregulated in the Model+M group (Fig. 2A and B, P<0.001) and also at the RNA level (Fig. 2F, P<0.001). These findings demonstrated that oxidative stress regulated the expression levels of apoptosis-related proteins (Bax, C-caspase-3, C-caspase-9 and Bcl-2), and high expression of miR-122-5p can partially counteract the trend.

High expression of miR-122-5p reduces the levels of ROS and MDA and mitochondrial depolarization, but increases the SOD level under H_2O_2 condition. The MDA content was significantly elevated (Fig. 3A, P<0.001) while the SOD content was significantly reduced in the Model group (Fig. 3B, P<0.01) as compared with these findings in the Blank group. However, the MDA content was significantly decreased (Fig. 3A, P<0.01) while the SOD content was significantly increased in the Model+M group (Fig. 3B, P<0.05), relative to the Model+MC group. According to DCFH-DA fluorescence detection of the ROS level in the HEI-OC1 cells, compared with the Blank group, the ROS level was significantly increased in the Model group (Fig. 3C and D, P<0.001); while compared to the Model + MC group, the ROS level was significantly reduced in the Model+M group (Fig. 3C and D, P<0.01). Mitochondrial membrane potential analysis indicated that the Model group had an significantly increased λ530/λ590 ratio relative to Blank group (P<0.001), while the Model+M group exhibited a statistically decreased λ530/λ590 ratio (P<0.001), when compared with that of the Model+MC group (Fig. 3E). The results above suggest that the high expression of miR-122-5p can partially reverse the oxidative damage of HEI-OC1 cells.

miR-122-5p directly targets FOXO3. TargetScan V7.2 (www.targetscan.org/vert_72/) predicted that miR-122-5p targets FOXO3 (Fig. 4A). The dual luciferase results showed that FOXO3-WT (wild-type) decreased luciferase activity in the M group compared to MC group (Fig. 4B, P<0.001), while FOXO3-MUT (mutated) had no significant changes. This demonstrated that miR-122-5p can directly target FOXO the 3'UTR (untranslated region) sequences (Fig. 4).

FOXO3 overexpression reverses the effects of miR-122-5p mimic on viability and apoptosis of H_2O_2-induced HEI-OC1 cells. WB and RT-qPCR assays demonstrated that the FOXO3 expression level was significantly increased in the Model group (Fig. 5A-C, P<0.05) after HEI-OC1 cells were treated with H_2O_2, compared with that in the Blank group. HEI-OC1 cell viability was determined by MTT assay, as depicted in Fig. 5D. At 24, 48, and 72 h after HEI-OC1 cells were transfected, the cell viability in the Model group was significantly lower than that of the Blank group (P<0.05); the cell viability in the Model+M group was significantly increased as compared with Model+MC group (P<0.001); the cell viability in the Model+FOXO3 group was significantly decreased compared with the Model+NC group (P<0.01), which was offset by miR-122-5p mimic (P<0.01). Flow cytometry was utilized to evaluate the apoptosis rate, as delineated in Fig. 5E. In the Model group, there was a significant increase in the apoptosis rate in comparison with the Blank group (P<0.001). In addition, the Model+M group exhibited a significant decrease in

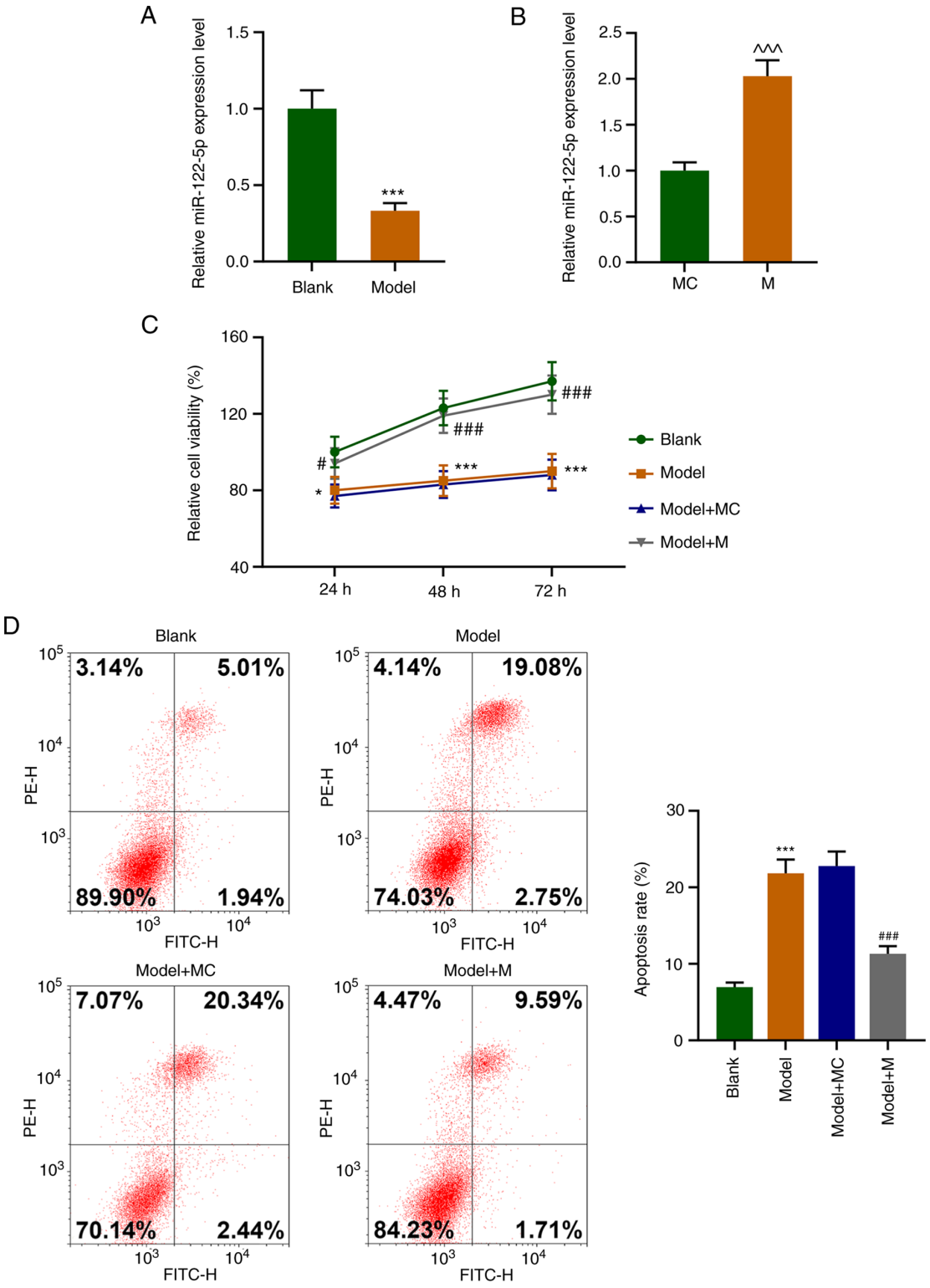

Figure 1. miR-122-5p increases the viability but inhibits the apoptosis of hydrogen peroxide (H_2O_2)-exposed HEI-OC1 cells. (A) Expression level of miR-122-5p in HEI-OC1 cells after oxidative damage of H_2O_2 (Model) was detected by reverse transcription quantitative polymerase chain reaction (RT-qPCR). ***P<0.001 vs. the Blank group. (B) Expression level of miR-122-5p in HEI-OC1 cells after transfection with the miR-122-5p mimic (M) or mimic control (MC) was detected by RT-qPCR. $^{\wedge\wedge\wedge}$P<0.001 vs. the MC group. (C) Viability of the HEI-OC1 cells following oxidative damage of H_2O_2 (Model) was determined by MTT assay in the different groups. $^{\#}$P<0.05 and $^{\#\#\#}$P<0.001 vs. the Model+MC group. *P<0.05 and ***P<0.001 vs. the Blank group. (D) Apoptosis of HEI-OC1 cells after oxidative damage of H_2O_2 was measured by flow cytometry in the different groups. ***P<0.001 vs. the Blank group; $^{\#\#\#}$P<0.001 vs. the Model + MC.

the apoptosis rate (P<0.01) as compared with Model+MC group. And compared with the Model+NC group, the apoptosis rate of cells in the Model+FOXO3 group was significantly increased (P<0.01). Moreover, the apoptosis rate of cells of the Model+M+FOXO3 group was notably lower than that in the Model+FOXO3 group (P<0.01). Moreover, in comparison with the Model+M group, the apoptosis rate of cells in the Model+M+FOXO3 group was dramatically elevated (P<0.01).

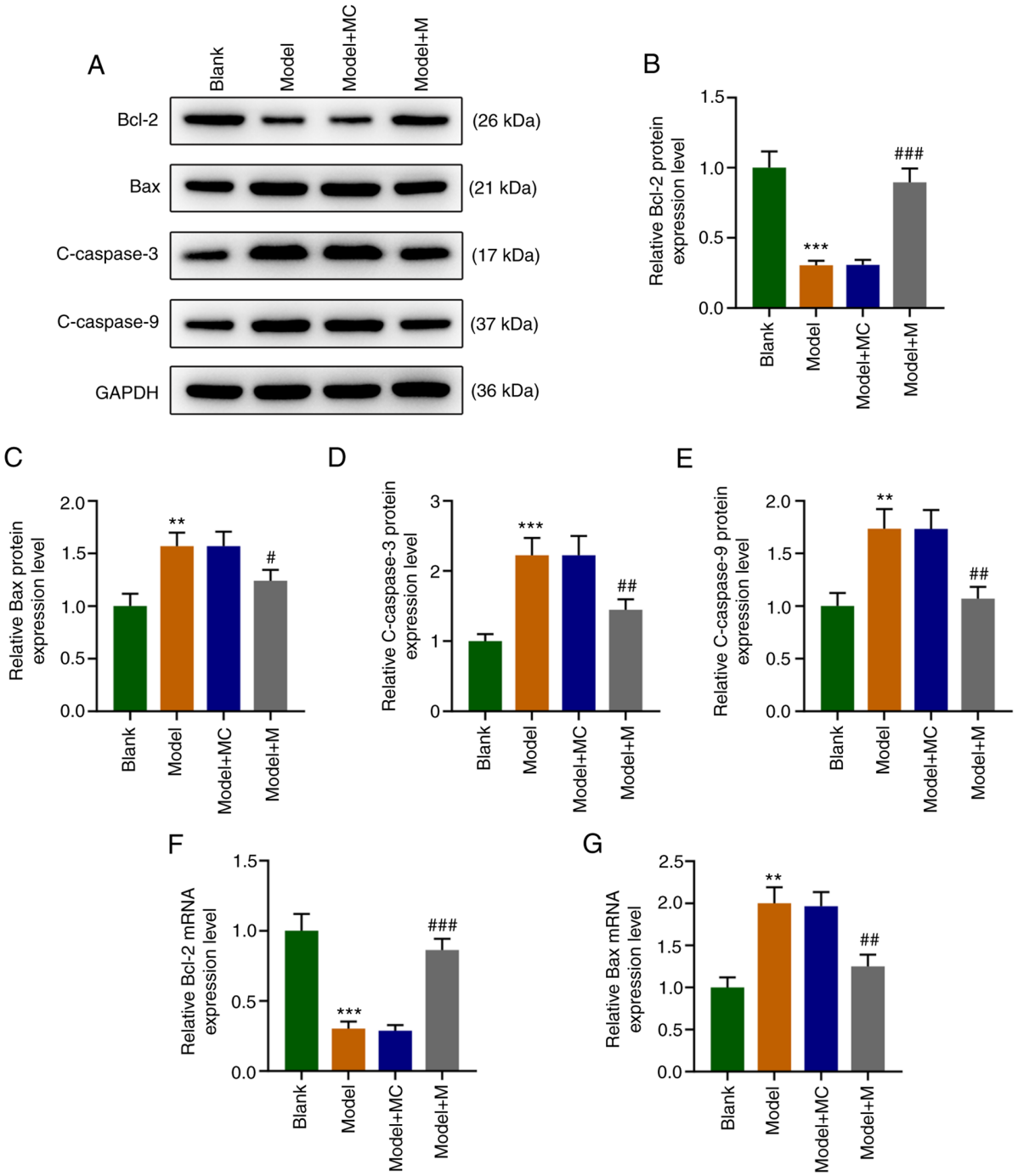

Figure 2. High expression of miR-122-5p can partially offset the effect of H_2O_2 on the expression levels of apoptotic molecules in HEI-OC1 cells. (A) Levels of Bcl-2, Bax, C-caspase-3 and C-caspase-9 in H_2O_2-induced HEI-OC1 cells were determined by western blot (WB) analysis. (B) Expression level of Bcl-2 in H_2O_2-induced HEI-OC1 cells was quantified by WB analysis. ***P<0.001 vs. the Blank group; $^{###}$P<0.001 vs. the Model+MC group. (C) Expression level of Bax in HEI-OC1 cells after oxidative damage of H_2O_2 was measured by WB analysis. **P<0.01 vs. the Blank group. $^{#}$P<0.05 vs. the Model+MC group. (D) Expression level of C-caspase-3 in H_2O_2-induced HEI-OC1 cells was tested by WB analysis. ***P<0.001 vs. the Blank group. $^{##}$P<0.01 vs. the Model+MC group. (E) Expression level of C-caspase-9 in H_2O_2-induced HEI-OC1 cells was detected by WB analysis. **P<0.01 vs. the Blank group. $^{##}$P<0.01 vs. the Model+MC group. (F) mRNA expression level of Bcl-2 in H_2O_2-induced HEI-OC1 cells was quantified by RT-qPCR. ***P<0.001 vs. the Blank group. $^{###}$P<0.001 vs. the Model+MC group. (G) mRNA expression level of Bax in H_2O_2-induced HEI-OC1 cells was determined by RT-qPCR. **P<0.01 vs. the Blank group. $^{##}$P<0.01 vs. the Model+MC group. Model, cells exposed to 50 μM H_2O_2 for 1 h; M, miR-122-5p mimic; MC, mimic control; C-, cleaved.

These above-mentioned findings indicated that FOXO3 overexpression overturned the effects of miR-122-5p mimic on viability and apoptosis of H_2O_2-induced HEI-OC1 cells.

FOXO3 overexpression reverses the effect of the miR-122-5p mimic on the expression levels of apoptosis-related molecules in H_2O_2-induced HEI-OC1 cells. Compared to the Blank group, the level of Bcl-2 was significantly decreased [at both the protein (Fig. 6A and B) and mRNA level (Fig. 6F), P<0.001], while the protein levels of Bax (and at the mRNA level as shown in Fig. 6G, P<0.01), C-caspase-3, and C-caspase-9 were significantly elevated in the Model group (Fig. 6A, C-E,

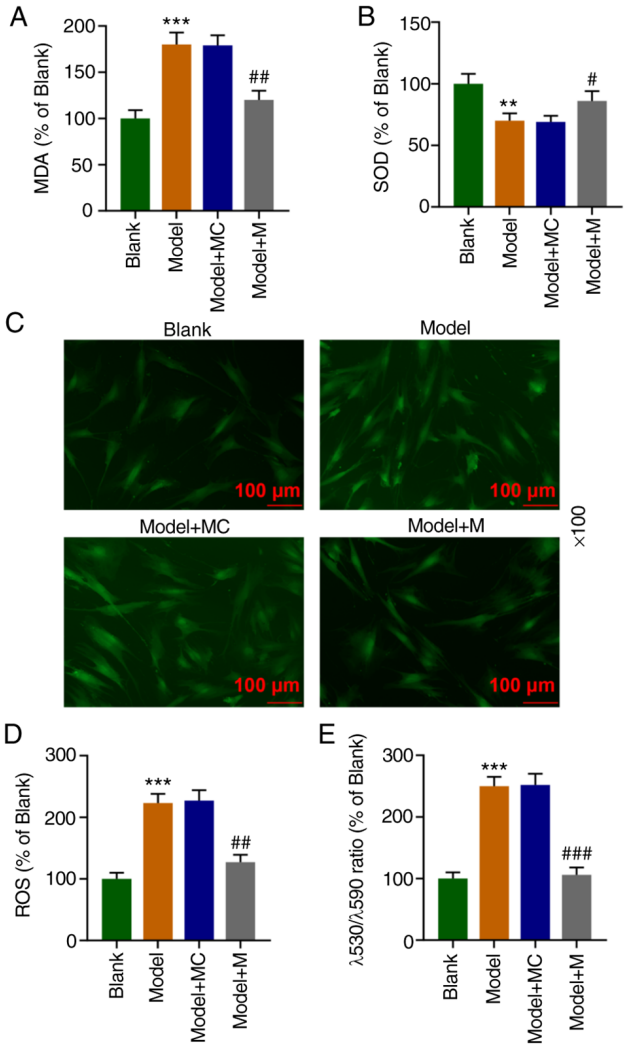

Figure 3. High expression of miR-122-5p reduces the levels of ROS and MDA and mitochondrial depolarization, but increases the SOD level under H_2O_2 condition. (A) MDA content in H_2O_2-induced HEI-OC1 cells was tested by enzyme-linked immunosorbent assay (ELISA). ***P<0.001 vs. the Blank group. $^{\#\#}$P<0.01 vs. the Model+MC group. (B) SOD content in H_2O_2-induced HEI-OC1 cells was evaluated by ELISA. **P<0.01 vs. the Blank group. $^{\#}$P<0.05 vs. the Model+MC group. (C and D) ROS content in H_2O_2-induced HEI-OC1 cells was determined by laser scanning confocal microscope. ***P<0.001 vs. the Blank group. $^{\#\#}$P<0.01 vs. the Model+MC group. (E) Cell membrane potential level in H_2O_2-induced HEI-OC1 cells was detected by flow cytometry. ***P<0.001 vs. the Blank group. $^{\#\#\#}$P<0.001 vs. the Model+MC group. Model, cells exposed to 50 μM H_2O_2 for 1 h; M, miR-122-5p mimic; MC, mimic control.

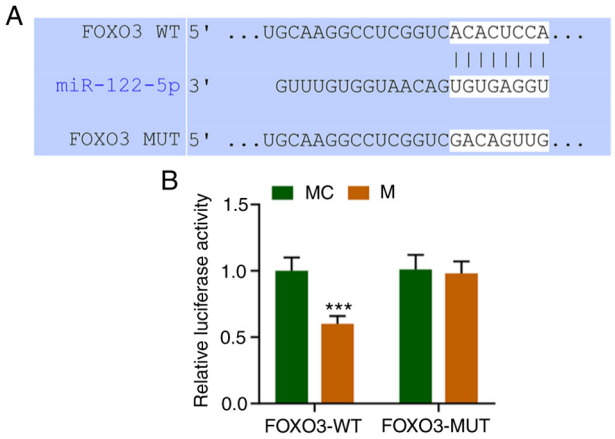

Figure 4. miR-122-5p directly targets FOXO3. (A) The 3'UTR sequences of FOXO3-wild-type (WT), FOXO3-mutant (MUT) and miR-122-5p. (B) Dual luciferase reporter assay was applied to analyze the fluorescence activity in H_2O_2-induced HEI-OC1 cells. ***P<0.001. vs. MC. FOXO3, forkhead box O3; M, miR-122-5p mimic; MC, mimic control.

P<0.001). As compared with Model+MC group, the expression levels of Bax (at the protein and mRNA levels), C-caspase-3 and C-caspase-9 in the Model+M group were significantly downregulated (Fig. 6A, C-E and G, P<0.01), whereas that of Bcl-2 was significantly upregulated [at the protein level as shown in Fig. A and B, P<0.001; at the mRNA level as shown in Fig. 6F, P<0.001). Relative to the Model+NC group, the level of Bcl-2 (at the protein level as shown in Fig. 6A and B, P<0.05; at the mRNA level as shown in Fig. 6F, P<0.05) was significantly decreased, while levels of Bax (at both the protein and mRNA levels), C-caspase-3, C-caspase-9 were significantly elevated in the Model+FOXO3 group (Fig. 6A, C-E and G, P<0.01). In contrast with the Model+FOXO3 group, the level of Bcl-2 was increased (both at the protein as shown in Fig. A and B; and the mRNA level as shown in Fig. 6F, P<0.05), while levels of Bax (at both the protein and mRNA level), C-caspase-3, and C-caspase-9 were significantly decreased in the Model+M+FOXO3 group (Fig. 6A, C-E and G, P<0.01). These data above indicated that FOXO3 overexpression counteracted the effects of miR-122-5p mimic on the expression levels of apoptosis-related proteins in H_2O_2-induced HEI-OC1 cells.

FOXO3 overexpression overturns the effect of miR-122-5p mimic on the levels of ROS, MDA, and SOD, and mitochondrial membrane depolarization in H_2O_2-induced HEI-OC1 cells. As compared with the Model+NC group, the levels of MDA (Fig. 7A), ROS (Fig. 7D) and λ530/λ590 ratio (Fig. 7E) were significantly increased in the Model+FOXO3 group (P<0.05), while the level of SOD (Fig. 7B) was significantly depleted (Fig. 7B, P<0.05). In comparison with the Model+FOXO3 group, the levels of MDA, ROS, together with λ530/λ590 ratio were significantly reduced in the Model+M+FOXO3 group (P<0.01), whereas the level of SOD was significantly elevated (Fig. 7A-D, P<0.01). These data suggested that FOXO3 overexpression neutralized the effects of miR-122-5p mimic on the levels of ROS, MDA, and SOD, and mitochondrial depolarization in H_2O_2-induced HEI-OC1 cells.

Discussion

In order to elucidate the regulatory mechanism of miR-122-5p on cochlear hair cells under oxidative stress, we established an oxidative stress model by exposing HEI-OC1 cells to 50 μM H_2O_2 for 1 h. The results of the present study were utilized to analyze the underlying role of miR-122-5p as a potential target for hearing loss treatment.

Under oxidative stress, reactive oxygen species (ROS) is a well-documented factor in noise-induced hearing loss. In several prior research studies, noise was found to activate AMPKα in outer hair cells (OHCs) through formation of ROS, and noise exposure-induced OHC death was mediated by a ROS/AMPKα-dependent pathway (24-26). High level of ROS

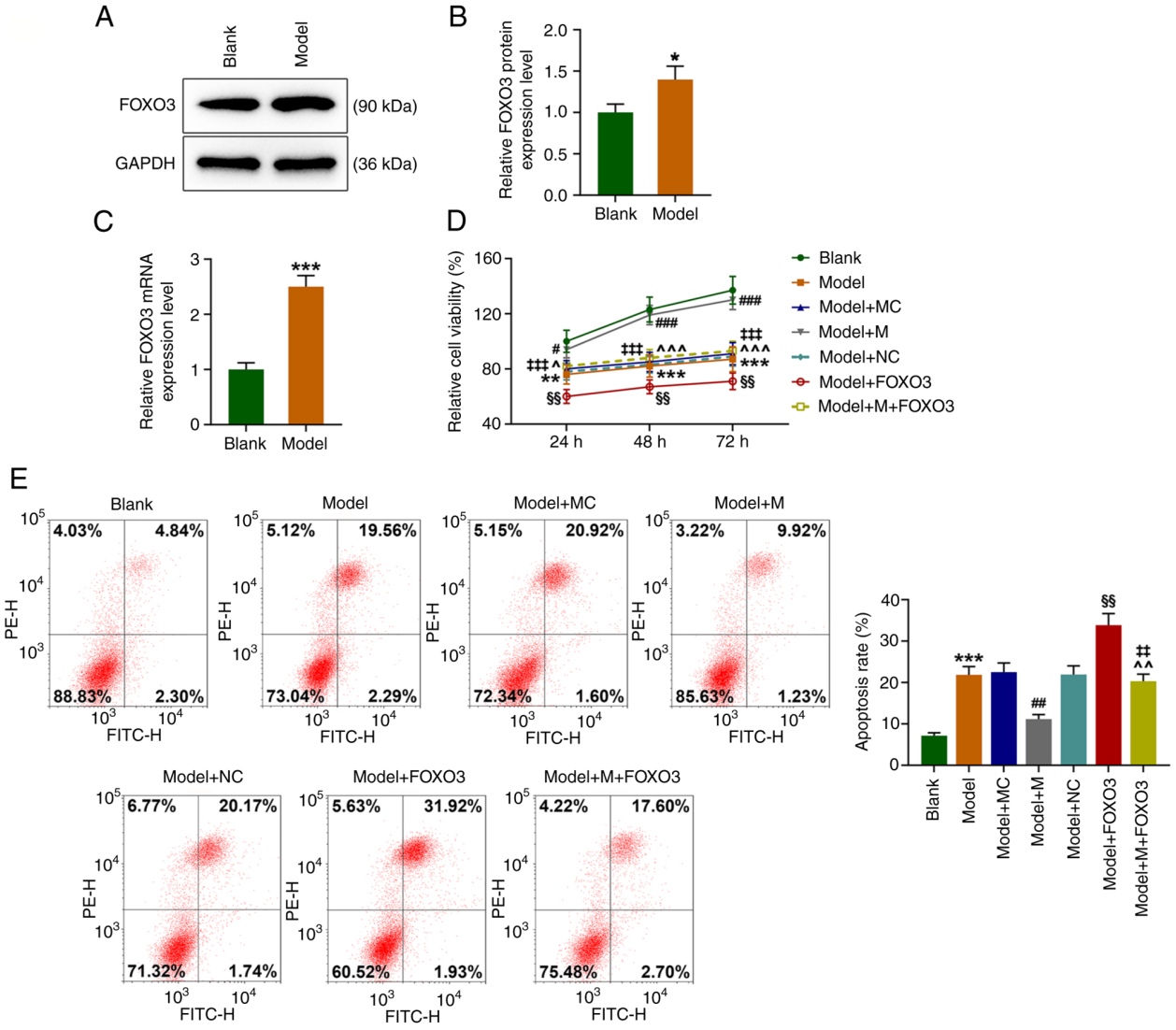

Figure 5. FOXO3 overexpression offsets the effects of miR-122-5p mimic (M) on viability and apoptosis of H_2O_2-induced HEI-OC1 cells. (A) Expression level of FOXO3 in H_2O_2-induced HEI-OC1 cells (Model) was measured by western blot analysis. (B) The protein expression level of FOXO3 in H_2O_2-induced HEI-OC1 cells was quantified by western blot analysis. *P<0.05 vs. the Blank group. (C) The mRNA expression level of FOXO3 in H_2O_2-induced HEI-OC1 cells was determined by RT-qPCR. ***P<0.001 vs. the Blank group. (D) Viability of the H_2O_2-induced HEI-OC1 cells in the different groups was evaluated by MTT assay. (E) Apoptosis of H_2O_2-induced HEI-OC1 cells was analyzed by flow cytometry. **P<0.01 and ***P<0.001 vs. the Blank group; $^{\#}$P<0.05, $^{\#\#}$P<0.01 and $^{\#\#\#}$P<0.001 vs. the Model+MC group; $^{\wedge}$P<0.05, $^{\wedge\wedge}$P<0.01 and $^{\wedge\wedge\wedge}$P<0.001 vs. the Model+M group; §§P<0.01 vs. the Model+NC group; ‡‡P<0.01 and ‡‡‡P<0.001 vs. the Model + FOXO3. Model, cells exposed to 50 μM H_2O_2 for 1 h; M, miR-122-5p mimic; MC, mimic control; NC, negative control; FOXO3, forkhead box O3.

is associated with hearing loss and hair cell death (2,27-29), which can cause changes in the expression levels of related proteins (30). Excess ROS overwhelms the redox balance and skews cell metabolism toward the activation of intrinsic apoptosis, which are regulated by the combined actions of pro- and anti-apoptotic members of the Bcl-2 family (31-34). It has been well established that the anti-apoptotic protein Bcl-2 can prevent the release of cytochrome *c* and reduce the activation of caspase-9 and caspase-3, thus inhibiting caspase-3-dependent apoptosis (30,35). Thus, the degree of oxidative stress can be identified in cells by assessing the expression levels of apoptotic proteins. Apoptosis, MDA production, SOD expression and changes in mitochondrial membrane potential can all be exploited to assess oxidation reactions (36,37). The results in this study signified that under oxidative stress, the cell viability was weakened and apoptosis was enhanced. With regard to the expression levels of apoptosis-related proteins, the Bcl-2 level was decreased, while those of Bax, cleaved (C)-caspase-3, and C-caspase-9 were elevated in HEI-OC1 cells. Additionally, the levels of ROS, MDA and the mitochondrial membrane potential were increased, yet the SOD level was reduced in the HEI-OC1 cells. Seminal miRNA-122 has been manifested to be negatively correlated with oxidative stress, and apoptotic markers (Bax, Bcl-2) in infertile men with varicocele (38). In the present study, the miR-122-5p level was found to be decreased in H_2O_2-induced HEI-OC1 cells, and miR-122-5p mimic was able to partially offset the effect of H_2O_2 on the cell viability and apoptosis, mitochondrial membrane potential levels, as well as apoptosis- and oxidative-related molecules in the HEI-OC1 cells. Taken together, miR-122-5p can attenuate H_2O_2-induced oxidative damage in HEI-OC1 cells.

In order to elucidate the possible mechanism of miR-122-5p on cochlear hair cells under oxidative stress, we gained access to the TargetScan V7.2 website to predict

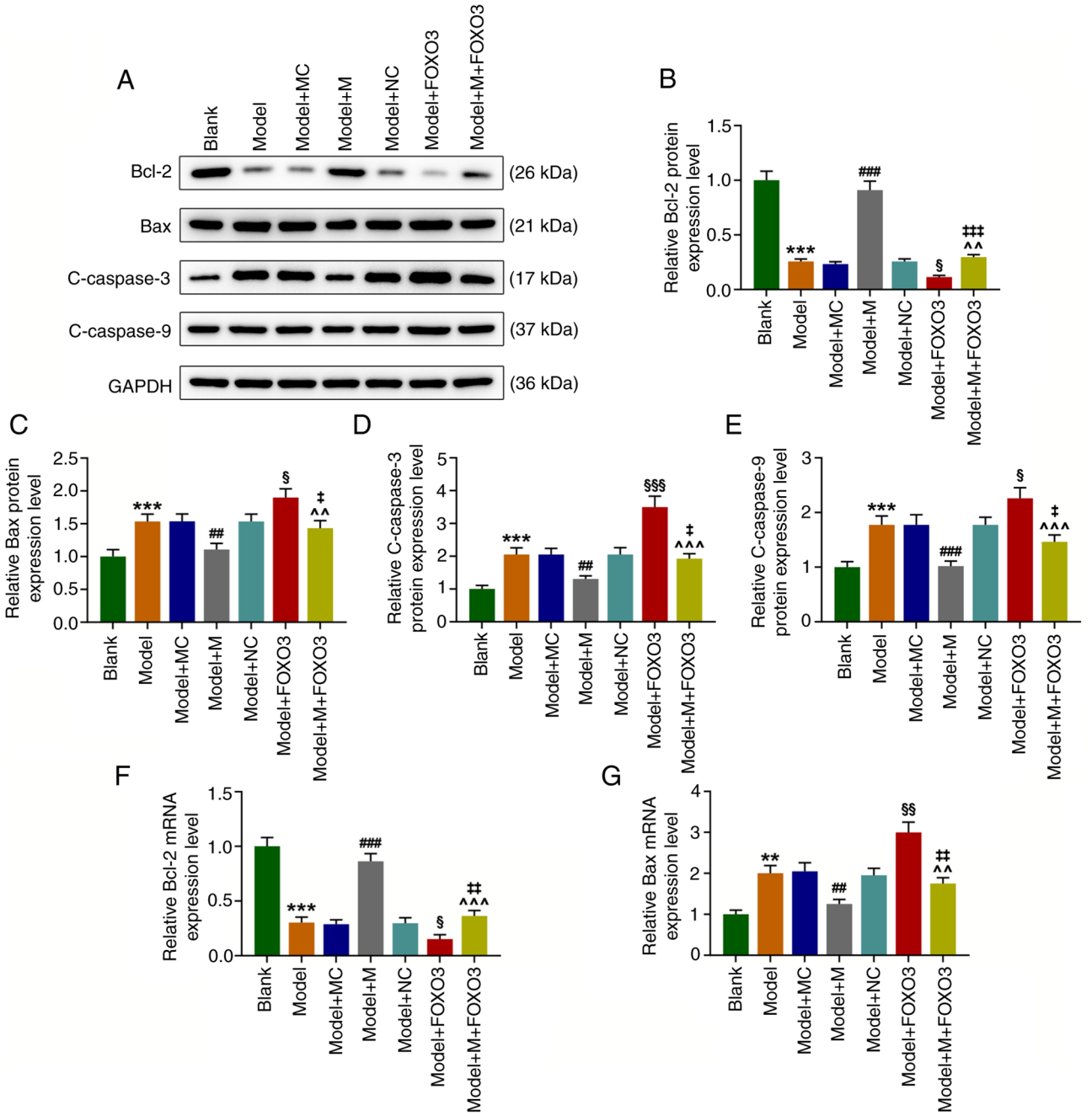

Figure 6. FOXO3 overexpression reverses the effect of miR-122-5p mimic on the expression levels of apoptosis-related proteins in H_2O_2-induced HEI-OC1 cells. (A) HEI-OC1 cells were transfected with miR-122-5p mimic (M), mimic control (MC), FOXO3 overexpression vector or negative control (NC), and the expression levels of Bcl-2, Bax, cleaved-caspase-3 and C-caspase-9 were detected by western blot (WB) analysis in HEI-OC1 cells after oxidative damage of H_2O_2. (B) The protein expression level of Bcl-2 was quantified by WB analysis in HEI-OC1 cells after oxidative damage of H_2O_2. (C) The protein expression level of Bax was measured by WB analysis in HEI-OC1 cells after oxidative damage of H_2O_2. (D) The protein expression level of C-caspase-3 in H_2O_2-induced HEI-OC1 cells was tested by WB analysis. (E) The expression level of C-caspase-9 in H_2O_2-induced HEI-OC1 cells was assessed by WB analysis. (F) The mRNA expression level of Bcl-2 in H_2O_2-induced HEI-OC1 cells was quantified by RT-qPCR. (G) The mRNA expression level of Bax in H_2O_2-induced HEI-OC1 cells was determined by RT-qPCR. **P<0.01 and ***P<0.001 vs. the Blank group; $^{\#\#}$P<0.01 and $^{\#\#\#}$P<0.001 vs. the Model+MC group; $^{\wedge\wedge}$P<0.01 and $^{\wedge\wedge\wedge}$P<0.001 vs. the Model+M group; §P<0.05, §§P<0.01 and and §§§P<0.001 vs. the Model+NC group; ‡P<0.05, ‡‡P<0.01 and ‡‡‡P<0.001 vs. the Model + FOXO3. Model, cells exposed to 50 μM H_2O_2 for 1 h; M, miR-122-5p mimic; MC, mimic control; NC, negative control; FOXO3, forkhead box O3 overexpression vector; C-, cleaved.

the targeting relationship between miR-122-5p and FOXO3. Forkhead box O3 (FOXO3) belongs to the forkhead box O (FOX) family (FKHRL1) that has a common structural motif, namely the 'forkhead box' or 'winged helix' domain that is responsible for binding to chromatin DNA in the nucleus of cells (39). FOXO proteins act as nuclear transcription factors that mediate the inhibitory action of insulin or insulin-like growth factor (IGF-1) on key functions in diverse pathways including cell metabolism, proliferation, differentiation, oxidative stress, cell survival and senescence, autophagy and aging in mammals (39). FOXO3 has important significance in the process of oxidative stress. In the process of self-eating due to oxidative stress, cytoplasmic STAT3 constitutively inhibits autophagy by sequestering EIF2AK2 as well as by

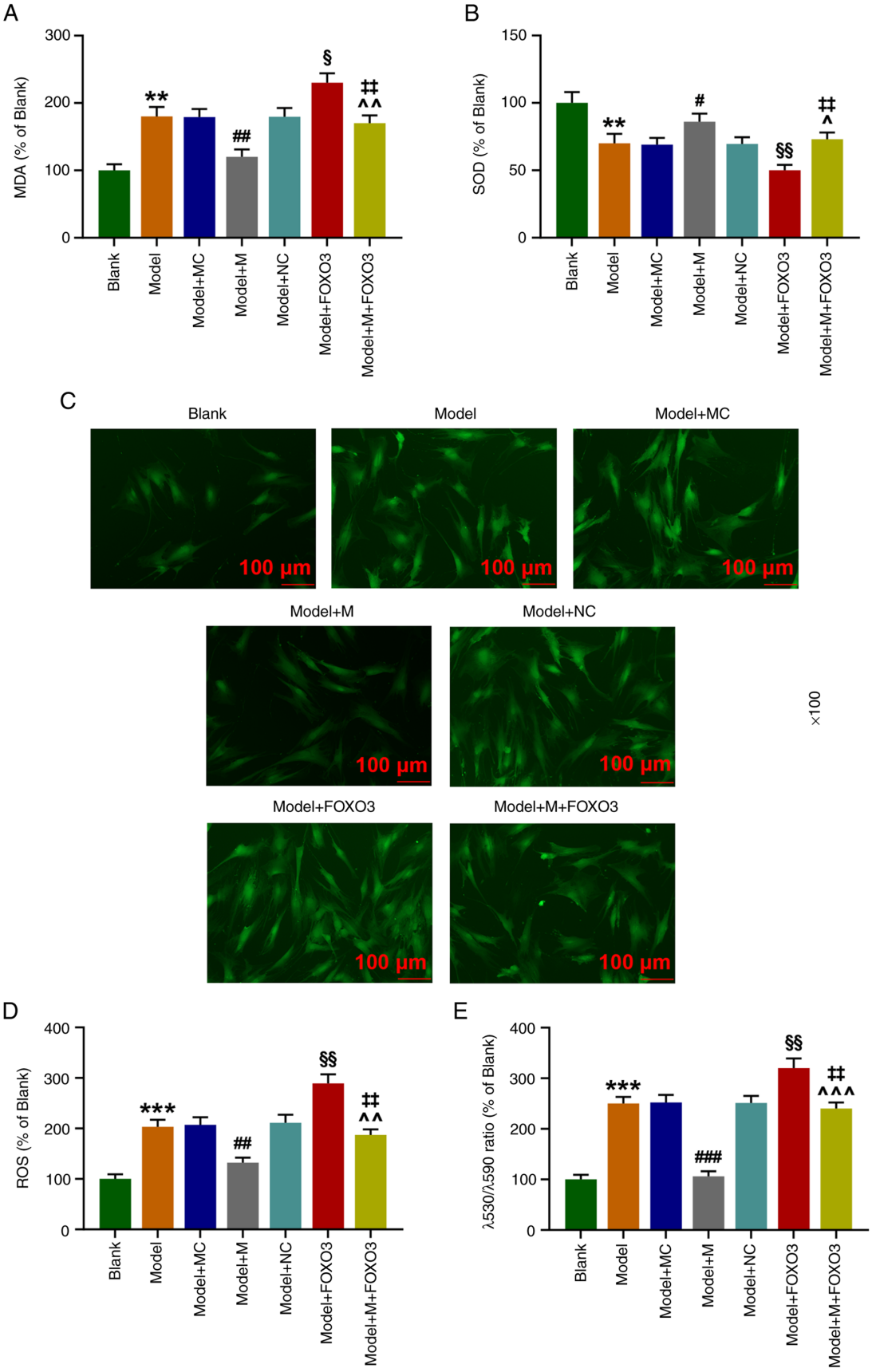

Figure 7. FOXO3 overexpression reverses the effects of miR-122-5p mimic on the levels of ROS, MDA, and SOD, and mitochondrial depolarization in H_2O_2-induced HEI-OC1 cells. (A) The content of MDA in transfected HEI-OC1 cells after oxidative damage of H_2O_2 was assessed by ELISA. (B) The content of SOD in transfected HEI-OC1 cells after oxidative damage of H_2O_2 was evaluated by ELISA. (C and D) ROS content of transfected HEI-OC1 cells after oxidative damage of H_2O_2 was detected by laser scanning confocal microscopy. (E) Cell membrane potential level of transfected HEI-OC1 cells after oxidative damage of H_2O_2 was determined by flow cytometry. **P<0.01 and ***P<0.001 vs. the Blank group; $^{\#}$P<0.05, $^{\#\#}$P<0.01 and $^{\#\#\#}$P<0.001 vs. the Model+MC group; $^{\wedge}$P<0.05, $^{\wedge\wedge}$P<0.01 and $^{\wedge\wedge\wedge}$P<0.001 vs. the Model+M group; §P<0.05 and §§P<0.01 vs. the Model+NC group; ‡‡P<0.01 vs. the Model + FOXO3. Model, cells exposed to 50 μM H_2O_2 for 1 h; M, miR-122-5p mimic; MC, mimic control; NC, negative control; FOXO3, forkhead box O3 overexpression vector.

interacting with other autophagy-related signaling molecules such as FOXO1 and FOXO3 (40). Increasing evidence demonstrates that multiple miRNAs can also synergistically act on FOXO3a, thus playing important roles in the development and progression of various human diseases (41-43). Additionally, overexpression of miR-182 represses the intrinsic apoptotic pathway by inhibiting the translation of FOXO3a, protecting cochlear hair cells from cisplatin-induced apoptosis in the inner ear (44). Gentamicin-induced cochlear hair cell ototoxicity, including oxidative stress and apoptosis, could be attenuated by mouse inner ear stem cells (IESCs) through the miR-182-5p/FOXO3 axis (45).

In the present study, it was found that the FOXO3 level was increased in H_2O_2-induced HEI-OC1 cells, and FOXO3 overexpression could further promote the effects of H_2O_2 on the viability and apoptosis, mitochondrial membrane potential levels, as well as apoptosis- and oxidative-related molecules in HEI-OC1 cells. In addition, the present findings also indicated that FOXO3 overexpression can partially offset the effect of high expression of miR-122-5p in H_2O_2-induced HEI-OC1 cells. Despite these achievements, our research still had some shortcomings. Only *in vitro* experiments, no *in vivo* experiments were conducted. The research also lacked a morphological basis. These should be explored in the further study. The above results illustrated that miR-122-5p can attenuate the H_2O_2-induced damage in mouse cochlear hair cells by targeting FOXO3.

In conclusion, the oxidative stress damage of hair cells caused by H_2O_2 can be alleviated by inhibiting the expression of FOXO3 or promoting the expression of miR-122-5p, providing a new perspective and scientific basis for the effective treatment of hearing impairment or loss.

Acknowledgements

Not applicable.

Funding

No funding was received.

Availability of data and materials

The analyzed datasets generated during the study are available from the corresponding author on reasonable request.

Authors' contributions

JC made substantial contributions to conception and design of the study. JQ and JL were responsible for the data acquisition, data analysis and interpretation and confirm the authenticity of all the raw data. JJ performed the drafting of the article and critically revised it for important intellectual content. All authors read and approved the final manuscript. All authors agree to be accountable for all aspects of the work in ensuring that questions related to the accuracy or integrity of the work are appropriately investigated and resolved.

Ethics approval and consent to participate

Not applicable.

Patient consent for publication

Not applicable.

Competing interests

The authors declare no competing interests.

References

1. Goutman JD, Elgoyhen AB and Gómez-Casati ME: Cochlear hair cells: The sound-sensing machines. FEBS Lett 589: 3354-3361, 2015.
2. Wang Z, Liu Y, Han N, Chen X, Yu W, Zhang W and Zou F: Profiles of oxidative stress-related microRNA and mRNA expression in auditory cells. Brain Res 1346: 14-25, 2010.
3. Burns JC and Stone JS: Development and regeneration of vestibular hair cells in mammals. Semin Cell Dev Biol 65: 96-105, 2017.
4. Bartel DP: MicroRNAs: Target recognition and regulatory functions. Cell 136: 215-233, 2009.
5. Vishnoi A and Rani S: MiRNA biogenesis and regulation of diseases: An overview. Methods Mol Biol 1509: 1-10, 2017.
6. Yao Q, Chen Y and Zhou X: The roles of microRNAs in epigenetic regulation. Curr Opin Chem Biol 51: 11-17, 2019.
7. Maruyama S, Furuya S, Shiraishi K, Shimizu H, Saito R, Akaike H, Hosomura N, Kawaguchi Y, Amemiya H, Kawaida H, *et al*: Inhibition of apoptosis by miR-122-5p in α-fetoprotein-producing gastric cancer. Oncol Rep 41: 2595-2600, 2019.
8. Wang W, Dong L, Zhao B, Lu J and Zhao Y: E-cadherin is downregulated by microenvironmental changes in pancreatic cancer and induces EMT. Oncol Rep 40: 1641-1649, 2018.
9. Byrnes CC, Jia W, Alshamrani AA, Kuppa SS and Murph MM: miR-122-5p expression and secretion in melanoma cells is amplified by the LPAR3 SH3-binding domain to regulate Wnt1. Mol Cancer Res 17: 299-309, 2019.
10. Xiong H, Pang J, Yang H, Dai M, Liu Y, Ou Y, Huang Q, Chen S, Zhang Z, Xu Y, *et al*: Activation of miR-34a/SIRT1/p53 signaling contributes to cochlear hair cell apoptosis: Implications for age-related hearing loss. Neurobiol Aging 36: 1692-1701, 2015.
11. Meng L, Chen Z, Jiang Z, Huang T, Hu J, Luo P, Zhang H, Huang M, Huang L, Chen Y, *et al*: MiR-122-5p suppresses the proliferation, migration, and invasion of gastric cancer cells by targeting LYN. Acta Biochim Biophys Sin (Shanghai) 52: 49-57, 2020.
12. Ding FN, Gao BH, Wu X, Gong CW, Wang WQ and Bio SM: miR-122-5p modulates the radiosensitivity of cervical cancer cells by regulating cell division cycle 25A (CDC25A). FEBS Open Bio 9: 1869-1879, 2019.
13. Cheng JL, Zhao H, Yang SG, Chen EM, Chen WQ and Li LJ: Plasma miRNA-122-5p and miRNA-151a-3p identified as potential biomarkers for liver injury among CHB patients with PNALT. Hepatol Int 12: 277-287, 2018.
14. Li DB, Liu JL, Wang W, Luo XM, Zhou X, Li JP, Cao XL, Long XH, Chen JG and Qin C: Plasma exosomal miRNA-122-5p and miR-300-3p as potential markers for transient ischaemic attack in rats. Front Aging Neurosci 10: 24, 2018.
15. Zhou F, Chen W, Cui Y, Liu B, Yuan Q, Li Z and He Z: miRNA-122-5p stimulates the proliferation and DNA synthesis and inhibits the early apoptosis of human spermatogonial stem cells by targeting CBL and competing with lncRNA CASC7. Aging (Albany NY) 12: 25528-25546, 2020.
16. Peng H, Luo Y and Ying Y: lncRNA XIST attenuates hypoxia-induced H9c2 cardiomyocyte injury by targeting the miR-122-5p/FOXP2 axis. Mol Cell Probes 50: 101500, 2020.
17. Rao L, Meng FL, Fang R, Cai CY and Zhao XL: Molecular mechanism of microRNA in regulating cochlear hair cell development. Yi Chuan 41: 994-1008, 2019 (In Chinese).
18. Xiong H, Chen S, Lai L, Yang H, Xu Y, Pang J, Su Z, Lin H and Zheng Y: Modulation of miR-34a/SIRT1 signaling protects cochlear hair cells against oxidative stress and delays age-related hearing loss through coordinated regulation of mitophagy and mitochondrial biogenesis. Neurobiol Aging 79: 30-42, 2019.
19. Wang JY, Xia Y, Yang CC and Wang Z: Analysis of microRNA regulatory network in cochlear hair cells with oxidative stress injury. Zhonghua Er Bi Yan Hou Tou Jing Wai Ke Za Zhi 51: 751-755, 2016 (In Chinese).

20. Li Y, Tang XL, Yu F, Li HJ and Yuan W: Expression and regulatory effect of miR-30b on dynamin in cochlear hair cells. Sichuan Da Xue Xue Bao Yi Xue Ban 49: 347-351, 2018 (In Chinese).
21. Zhou W, Du J, Jiang D, Wang X, Chen K, Tang H, Zhang X, Cao H, Zong L, Dong C and Jiang H: microRNA-183 is involved in the differentiation and regeneration of Notch signaling-prohibited hair cells from mouse cochlea. Mol Med Rep 18: 1253-1262, 2018.
22. Li Y, Li A, Wu J, He Y, Yu H, Chai R and Li H: MiR-182-5p protects inner ear hair cells from cisplatin-induced apoptosis by inhibiting FOXO3a. Cell Death Dis 7: e2362, 2016.
23. Tsuchihashi NA, Hayashi K, Dan K, Goto F, Nomura Y, Fujioka M, Kanzaki S, Komune S and Ogawa K: Autophagy through 4EBP1 and AMPK regulates oxidative stress-induced premature senescence in auditory cells. Oncotarget 6: 3644-3655, 2015.
24. Wu F, Xiong H and Sha S: Noise-induced loss of sensory hair cells is mediated by ROS/AMPKα pathway. Redox Biol 29: 101406, 2020.
25. Henderson D, Mcfadden SL, Liu CC, Hight N and Zheng XY: The role of antioxidants in protection from impulse noise. Ann N Y Acad Sci 884: 368-380, 1999.
26. Ohlemiller KK, Wright JS and Dugan LL: Early elevation of cochlear reactive oxygen species following noise exposure. Audiol Neurootol 4: 229-236, 1999.
27. Guthrie OW: Aminoglycoside induced ototoxicity. Toxicology 249: 91-96, 2008.
28. Henderson D, Bielefeld EC, Harris KC and Hu BH: The role of oxidative stress in noise-induced hearing loss. Ear Hear 27: 1-19, 2006.
29. Sugahara K, Rubel EW and Cunningham LL: JNK signaling in neomycin-induced vestibular hair cell death. Hear Res 221: 128-135, 2006.
30. Yu X, Liu W, Fan Z, Qian F, Zhang D, Han Y, Xu L, Sun G, Qi J, Zhang S, *et al*: c-Myb knockdown increases the neomycin-induced damage to hair-cell-like HEI-OC1 cells in vitro. Sci Rep 7: 41094, 2017.
31. Xie J, Talaska AE and Schacht J: New developments in aminoglycoside therapy and ototoxicity. Hear Res 281: 28-37, 2011.
32. Mangiardi DA, McLaughlin-Williamson K, May KE, Messana EP, Mountain DC and Cotanche DA: Progression of hair cell ejection and molecular markers of apoptosis in the avian cochlea following gentamicin treatment. J Comp Neurol 475: 1-18, 2004.
33. Coffin AB, Rubel EW and Raible DW: Bax, Bcl2, and p53 differentially regulate neomycin- and gentamicin-induced hair cell death in the zebrafish lateral line. J Assoc Res Otolaryngol 14: 645-659, 2013.
34. Fetoni AR, Paciello F, Rolesi R, Paludetti G and Troiani D: Targeting dysregulation of redox homeostasis in noise-induced hearing loss: Oxidative stress and ROS signaling. Free Radic Biol Med 135: 46-59, 2019.
35. Green DR and Reed JC: Mitochondria and apoptosis. Science 281: 1309-1312, 1998.
36. Wang Z, Yu J, Wu J, Qi F, Wang H, Wang Z and Xu Z: Scutellarin protects cardiomyocyte ischemia-reperfusion injury by reducing apoptosis and oxidative stress. Life Sci 157: 200-207, 2016.
37. Wu X, Li X, Song Y, Li H, Bai X, Liu W, Han Y, Xu L, Li J, Zhang D, *et al*: Allicin protects auditory hair cells and spiral ganglion neurons from cisplatin-Induced apoptosis. Neuropharmacology 116: 429-440, 2017.
38. Mostafa T, Rashed LA, Nabil NI, Osman I, Mostafa R and Farag M: Seminal miRNA relationship with apoptotic markers and oxidative stress in infertile men with varicocele. Biomed Res Int 2016: 4302754, 2016.
39. Accili D and Arden KC: FoxOs at the crossroads of cellular metabolism, differentiation, and transformation. Cell 117: 421-426, 2004.
40. You L, Wang Z, Li H, Shou J, Jing Z, Xie J, Sui X, Pan H and Han W: The role of STAT3 in autophagy. Autophagy 11: 729-739, 2015.
41. Yang N, Zhang Q and Bi XJ: MiRNA-96 accelerates the malignant progression of ovarian cancer via targeting FOXO3a. Eur Rev Med Pharmacol Sci 24: 65-73, 2020.
42. Zhang J, Xu H, Gong L and Liu L: MicroRNA-132 protects H9c2 cells against oxygen and glucose deprivation-evoked injury by targeting FOXO3A. J Cell Physiol 235: 176-184, 2020.
43. Yao RD, Li HL, Liu Y and Sun LT: MiRNA-1 promotes pyroptosis of cardiomyocytes and release of inflammatory factors by downregulating the expression level of PIK3R1 through the FoxO3a pathway. Eur Rev Med Pharmacol Sci 24: 11243-11250, 2020.
44. Ran X, Li Y, Chen G, Fu S, He D, Huang B, Wei L, Lin Y, Guo Y and Hu G: Farrerol ameliorates TNBS-induced colonic inflammation by inhibiting ERK1/2, JNK1/2, and NF-κB signaling pathway. Int J Mol Sci 19: 2037, 2018.
45. Lai R, Cai C, Wu W, Hu P and Wang Q: Exosomes derived from mouse inner ear stem cells attenuate gentamicin-induced ototoxicity in vitro through the miR-182-5p/FOXO3 axis. J Tissue Eng Regen Med 14: 1149-1156, 2020.